17. Richards, M. A., Ricard, Y., Lithgow-Bertelloni, C., Spada, G. & Sabadini, R. An explanation for Earth's long-term rotational stability. *Science* **275,** 372–375 (1997).
18. Spada, G., Ricard, Y. & Sabadini, R. Excitation of true polar wander by subduction. *Nature* **360,** 452–454 (1992).
19. Forte, A. M., Woodward, R. L. & Dziewonski, A. M. Joint inversions of seismic and geodynamic data for models of three-dimensional mantle heterogeneity. *J. Geophys. Res.* **99,** 21857–21877 (1994).
20. Karato, S.-I. Importance of anelasticity in the interpretation of seismic tomography. *Geophys. Res. Lett.* **20,** 1623–1626 (1993).
21. Forte, A.M., Mitrovica, J.X. & Woodward, R.L. Seismic-geodynamic determination of the origin of excess ellipticity of the core-mantle boundary. *Geophys. Res. Lett.* **22,** 1013–1016 (1995).
22. Mitrovica, J. X. & Forte, A. M. Radial profile of mantle viscosity: results from the joint inversion of convection and postglacial rebound observations. *J. Geophys. Res.* **102,** 2751–2769 (1997).
23. Imbrie, J. Astronomical theory of the Pleistocene ice ages: A brief historical review. *Icarus* **50,** 408–422 (1982).
24. Lourens, L. J. *et al*. Evaluation of the Plio-Pleistocene astronomical timescale. *Paleoceanography* **11,** 391–413 (1996).
25. Néron de Surgy, O. & Laskar, J. On the long term evolution of the spin of the Earth. *Astron. Astrophys.* **318,** 975–989 (1997).
26. Forte, A. M., Dziewonski, A. M. & Woodward, R. L. Aspherical structure of the mantle, tectonic plate motions, nonhydrostatic geoid, and topography of the core–mantle-boundary, in *Dynamics of the Earth's Deep Interior and Earth Rotation* (ed. Le-Mouel, J.-L., Smylie, D. E. & Herring, T.) 135–166 (Geophys. Monogr. 72, AGU, Washington, DC, 1993).
27. Li, X.-D. & Romanowicz, B. Global mantle shear-velocity model developed using nonlinear asymptotic coupling theory. *J. Geophys. Res.* **101,** 22245–22272 (1996).
28. Masters, G., Johnson, S., Laske, G. & Bolton, H. A shear-velocity model of the mantle. *Phil. Trans. R. Soc. Lond. A* **354,** 1385–1411 (1996).

Acknowledgements. We thank J. Laskar for making available his orbital integration codes. A.M.F. thanks his colleagues for discussions, in particular J. Laskar (Bureau des Longitudes), A. Pais (IPGP) and J.-L. LeMouel (IPGP). J.X.M was supported in part by NSERC and also by the Canadian Institute for Advanced Research (Earth Systems Evolution Program).

Correspondence should be addressed to A.M.F. (e-mail: forte@ipgp.jussieu.fr).

Regeneration of adult axons in white matter tracts of the central nervous system

Stephen J. A. Davies*†, Michael T. Fitch*, Stacey P. Memberg*, Alison K. Hall*, Geoffrey Raisman† & Jerry Silver*

** Department of Neurosciences, Case Western Reserve University School of Medicine, 10900 Euclid Avenue, Cleveland, Ohio 44106, USA*
† Norman & Sadie Lee Research Centre, Division of Neurobiology, National Institute for Medical Research, London NW7 1AA, UK

It is widely accepted that the adult mammalian central nervous system (CNS) is unable to regenerate axons[1]. In addition to physical or molecular barriers presented by glial scarring at the lesion site[2–4], it has been suggested that the normal myelinated CNS environment contains potent growth inhibitors[5,6] or lacks growth-promoting molecules[1,7]. Here we investigate whether adult CNS white matter can support long-distance regeneration of adult axons in the absence of glial scarring, by using a microtransplantation technique[8] that minimizes scarring[9] to inject minute volumes of dissociated adult rat dorsal root ganglia directly into adult rat CNS pathways. This atraumatic injection procedure allowed considerable numbers of regenerating adult axons immediate access to the host glial terrain, where we found that they rapidly extended for long distances in white matter, eventually invading grey matter. Abortive regeneration correlated precisely with increased levels of proteoglycans within the extracellular matrix at the transplant interface, whereas successfully regenerating transplants were associated with minimal upregulation of these molecules. Our results demonstrate, to our knowledge for the first time, that reactive glial extracellular matrix at the lesion site is directly associated with failure of axon regrowth *in vivo*, and that adult myelinated white matter tracts beyond the glial scar can be highly permissive for regeneration.

Previous studies have demonstrated that embryonic axons can grow long distances within adult CNS white matter[8–10], but it was considered that embryonic neurons might possess a superior intrinsic axon growth potential compared with adult neurons, or that they had not yet acquired receptors for myelin inhibitors (M. E. Schwab, personal communication). Thus, the question remained as to whether adult white matter could be an inherently conducive highway for axon regeneration from an adult neuron in the absence of glial scarring. We used a microtransplantation technique[8] to address this question by injecting 0.5-μl volumes of dissociated suspensions of either adult or postnatal-day-eight (P8) dorsal root ganglia (DRG) neurons and accompanying satellite cells directly into the white matter of the corpus callosum ($n = 25$) or the fimbria ($n = 16$) (Fig. 1). Transplanted DRG neurons were used for the following reasons: (1) a subpopulation maintains high levels of calcitonin-gene-related peptide (CGRP) following transplantation and can be readily distinguished from the CGRP-negative axons of the host corpus callosum and fimbria; (2) DRG neurons (including the CGRP-containing population) will not regenerate their axons within the CNS beyond the second postnatal day[11,12]; (3) examination of transplanted neurons avoids the complications of axonal sparing associated with crush or partial injury paradigms; and (4) it has been shown that DRGs are inhibited *in vitro* by mature oligodendrocytes or CNS myelin components[13,14], and our observations verify this finding for the adult CGRP-positive subpopulation (data not shown).

Fluorescent immunolabelling for CGRP at 2 days ($n = 4$ adults) post-transplantation showed intense staining of a subset of DRG neuronal cell bodies which had extended two or three minor processes (<20 μm) that resembled filopodia and one longer axonal process with a growth cone of simple morphology. Axons

Table 1 No. of adult donor CGRP⁺ neurons and their regenerating axons

Survival time	Identification no.	A	B	C
2 days	V49	60	2	0
	V50	51	0	0
4 days	V9	108	39	15
	V10	130	41	16
	V11	75	28	10
	V51	117	35	12
6 days	V43	110	38	32
	V44	116	40	31
	V54	94	32	27
	V55	81	27	21

Contralaterally directed regenerating axons from individual successful intracallosal grafts were counted through adjacent 60-μm horizontal sections within callosal white mater at the midline, and from the contralateral rostrum callosal white matter at its interface with overlying cortical grey matter. Columns: A, numbers of CGRP⁺ neuronal cell bodies in intracallosal grafts; B, numbers of axons at midline of corpus callosum; C, numbers of axons at contralateral white/grey matter interface. Average number of CGRP⁺ neuronal cell bodies, 94; average number of axons at midline, 35 (4- and 6-day combined); average number of axons at contralateral white/grey matter interface at 2 d, 0; at 4 d, 13.3; at 6 d, 27.7.

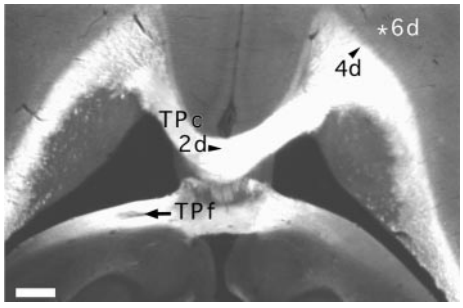

Figure 1 Photomicrograph of an unstained 60-μm horizontal section through an adult rat brain indicating microtransplant locations and maximum distances for adult axon regeneration from intracallosal grafts at 2 (2d, arrowhead), 4 (4d, arrowhead) and 6 (*6d) days post-transplantation. The ovoid transplants were ~1 mm long by 0.5 mm wide. The light-reflective properties of the myelinated white matter tracts contrast with the transplant seen easily in the fimbria in this section. TPc, transplant position in corpus callosum. Tpf (arrow), transplant position in fimbria. Scale bar, 1 mm.

varied in length, some having already entered the host tract as far as 0.5 to 2 mm away from the edge of the transplants, whereas others had only ventured little more than 100 μm into the host white matter. By 4 days post-transplantation ($n = 18$ transplants total), large numbers of CGRP-positive axons from P8 ($n = 6$ successful transplants) and adult ($n = 7$ successful transplants) DRG microtransplants crossed the graft/host interface and extended contralaterally for maximum distances of ~6 mm (Figs 1, 2a). Axons always exited in about equal numbers from clearly defined departure points at either pole of the ovoid-shaped transplants which were in continuity with host-tract glial structures (Fig. 3a, c). Once out of the graft territory and into host white matter, donor axons did not appear to fasciculate with each other and lacked collaterals (Fig. 2a). Regenerating axons exhibited 'bullet-shaped' growth cones (Fig. 2b) with a single leading filopodium, resembling those previously observed within developing CNS pathways where axons were growing in a rapid and uninhibited fashion[15]. Double staining for CGRP and a myelin-specific antigen showed that the growing

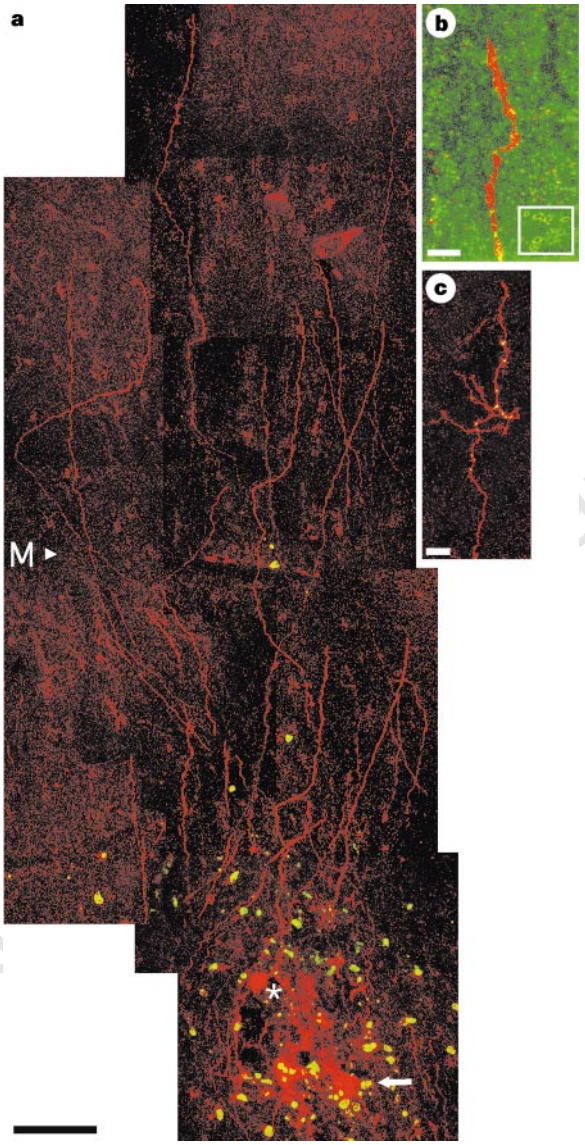

Figure 2 Regenerating adult DRG axons in adult rat corpus callosum. **a**, Confocal montage of a portion of an intracallosal adult DRG microtransplant scanned through two adjacent 60-μm horizontal sections. $CGRP^+$ donor adult axons (red) exit the graft and extend within host white matter to cross the midline (M, arrowhead) to enter the contralateral hemisphere. Satellite cells (p75; green) were associated with donor neuron cell bodies (an example is indicated by the arrow) but not with axons. The asterisk indicates a $CGRP^+$ donor neuron near the transplant interface with host white matter (see also Fig. 3c). Survival, 4 days; scale bar 100 μm. **b**, High-power confocal image through 17 μm of tangentially sectioned tissue showing a $CGRP^+$ (red) adult donor axon with a streamlined growth cone extending through the myelin-rich (CNS myelin-specific mAb 328; green) adult host callosum, 2.5 mm from the graft. Inset: low-power image of mAb 328 immunohistochemistry shows typical myelin rings when white matter is cut in cross-section. Survival, 4 days; scale bar, 10 μm. **c**, Confocal image of a donor adult $CGRP^+$ axon terminal within host cortical grey matter. Survival, 6 days; scale bar, 50 μm.

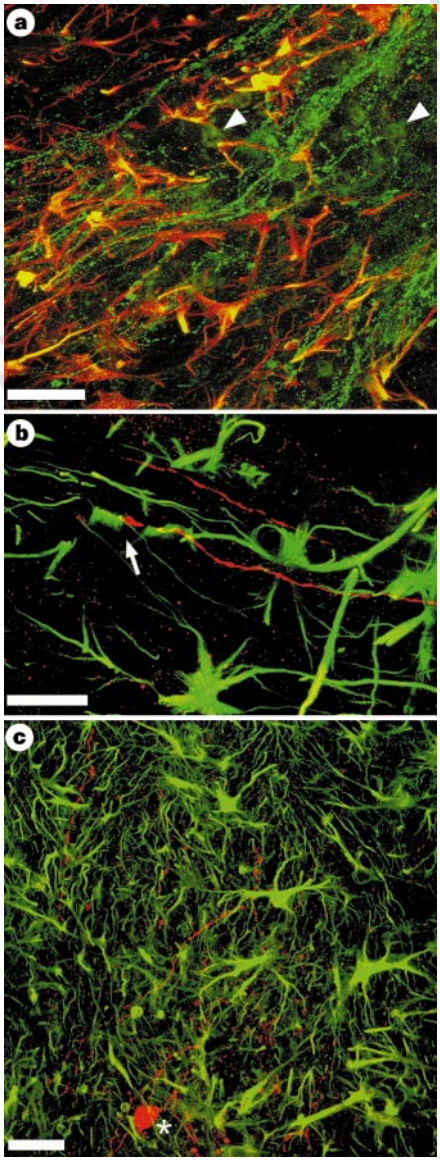

Figure 3 Transplant integration and association of regenerating axons with host astrocytes. **a**, Confocal image (60 μm) showing regenerating CGRP-positive P8 axons (green) associated with GFAP-positive astrocytes (red) in the adult fimbria. Large numbers of axons are exiting the transplant (top right) and growing in close association with astrocyte processes in white matter. Arrowheads indicate examples of faintly stained CGRP-positive neuron cell bodies. Survival, 4 days; scale bar, 20 μm. **b**, Confocal image (20 μm) showing adult donor DRG CGRP-positive axons (red) extending through white matter of the adult host fimbria. A growth cone of a regenerating axon (arrow) is closely aligned with the GFAP-positive (green) longitudinal processes of the host adult white-matter astrocytes. Survival, 2 days; scale bar, 20 μm. **c**, Confocal image (60 μm) of the same adult donor intracallosal transplant shown in Fig. 2a restained for GFAP (green). Asterisk marks the same CGRP-positive neuron (red) shown in Fig. 2a. The transplant is completely integrated with no readily definable interface between the graft and host tissue. Survival, 4 days; scale bar, 50 μm.

tips of the adult axons were extending through white matter with a normal myelin content (Fig. 2b). At 6 days ($n = 6$ successful transplants), donor axons could be seen exiting the callosum in both hemispheres to enter host prefrontal cortex, a distance contralaterally of 6–7 mm from the transplant boundary (Fig. 1) and 2–3 mm ipsilaterally. Some of the donor axons had now branched to form simple terminal arbors, suggesting innervation of host grey matter (Fig. 2c). Putative regenerated terminals were confirmed to be continuous with axons leading back to the transplant. Counts of CGRP-positive neurons and their axons within host white matter from successful adult donor grafts at 4 and 6 days combined show that on average 35% of CGRP-positive neurons had projected axons across the midline of the callosum (Table 1). Furthermore, 80% of these axons at the midline had reached the contralateral white–grey matter interface of the rostrum of the corpus callosum at 6 days (Table 1). Ipsilaterally projecting axons were not quantified owing to the close proximity of some grafts to ipsilateral host grey matter. Control sections from normal animals ($n = 2$), or those with only micropipette stabs ($n = 2$), showed no immunoreactivity for CGRP in the callosum or fimbria. No differences were observed in either the speed or extent of regenerative growth achieved by adult or P8 donor axons, results that are virtually identical to those described for embryonic CNS neurons microtransplanted in a similar fashion[8,9].

At 8 days survival ($n = 11$), CGRP immunoreactivity of axons and cell bodies had downregulated in all transplants. Immunostaining for peripherin showed that significant numbers of DRG neurons were still present within the transplant neuropil, suggesting that CGRP downregulation may be an active rather than a degenerative process. Peripherin immunohistochemistry could not be used as an unequivocal marker of regenerating DRG axons because of overlap with staining of resident axons in the forebrain.

Immunohistochemistry (using an antibody raised against antigen p75) for satellite cells[16] accompanying the donor DRG neurons showed no apparent association between these cells and CGRP-positive donor axons, as the growing tips of axons were far in advance of these slowly migrating glia in host white matter (Fig. 2a). Therefore it is unlikely that the satellite cells are modifying the entire length of the CNS pathways to make them more permissive for axon regeneration. However, the satellite cells may be critical for inducing regenerative outgrowth from transplants by modifying the graft/host interface, or by augmenting trophic support of the regenerating neurons. Reducing satellite cells to lower levels still allowed for robust DRG regeneration, and even at high levels their presence was insufficient to promote axon growth in those transplants that failed to regenerate. DRG neurons were only weakly immunoreactive for p75 (ref. 17).

Transplants exhibiting robust axon regeneration into adult white matter at 2, 4 and 6 days post-transplantation had very low levels of chondroitin-6-sulphate proteoglycan in matrix at the graft/host interface, with only light staining surrounding donor neuronal cell bodies (data not shown). There was a striking upregulation of proteoglycan staining at the boundaries of those transplants ($n = 7$) whose axons failed to enter the adjacent host white matter. Double staining for CGRP and proteoglycans in these transplants at 4 and 6 days showed axons that had stopped within the proteoglycan-rich boundaries or had actively turned away from the boundary and looped back into the transplant interior (Fig. 4a). A number of proteoglycans inhibit axon growth *in vitro*[18,19] and *in vivo* their upregulation coincides developmentally with the age beyond which the CNS fails to support axon regeneration[20,21]. These previous observations, taken together with our results, strongly suggest a potent role for reactive extracellular matrix in causing regeneration failure in the adult brain. However, we do not know at present which specific components of the matrix are crucial for axon repulsion. There are many different types of inhibitory proteoglycans[22] and in addition there may be other classes of inhibitors[23,24] co-localized within the barrier.

The molecules that trigger upregulation of proteoglycan-rich matrix are unknown and their characterization may help in developing therapeutic interventions. The smooth-edged, oval geometry of the proteoglycan border around failed transplants, coupled with

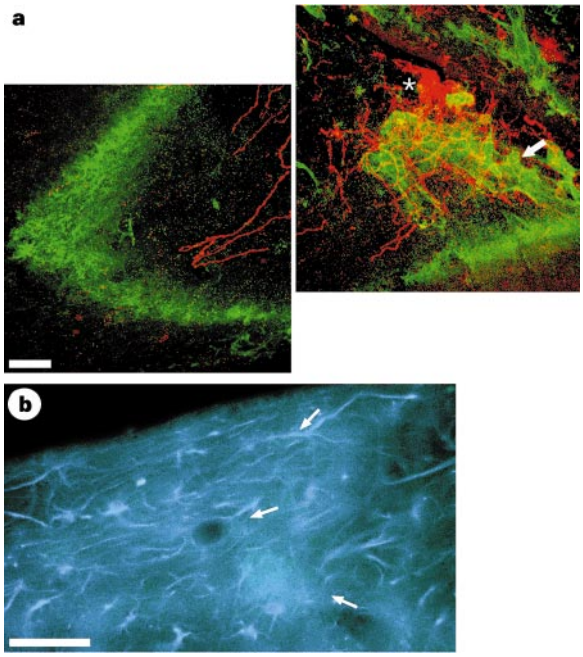

Figure 4 Regeneration failure associated with a proteoglycan boundary in the absence of a physical glial scar. **a**, Confocal images from the same 60-μm section of an adult intrafimbrial transplant that failed to regenerate. CGRP-positive axons (red) grew within the transplant but did not cross the proteoglycan-rich extracellular matrix boundary (green) which encapsulates the transplant. Proteoglycan was also deposited around blood vessels but only within the transplant (arrow). Asterisk denotes $CGRP^+$ neuron cell bodies. Survival, 4 days; scale bar, 50 μm. **b**, Fluorescent photomicrograph (not confocal) of the 60-μm section shown in **a**, immunostained for GFAP (AMCA; blue). Astrocytes are aligned and continuous across the graft/host interface; their morphology does not predict the location of the inhibitory proteoglycan boundary (arrows). Scale bar, 100 μm.

the presence of reactive, matrix-coated vessels within these grafts (Fig. 4a), suggests that a local breakdown of the blood–brain barrier precedes regeneration failure. The resulting intraparenchymal diffusion of serum borne factors could, in turn, trigger the production of inflammatory cytokines[25], as well as the reactive glial response leading to increased matrix production[26].

Staining for glial fibrillary acidic protein (GFAP) showed that in all transplants, even those with little or no outgrowth of axons across the proteoglycan-rich boundary, longitudinal astrocytic processes were aligned and in continuity from the host tract deep into the transplant neuropil (Figs 3c, 4b). We have also found that proteoglycans are distributed precisely in the region of neurite dystrophy observed in the microlesion model of axon-regeneration failure (unpublished observations), where cut adult axons again fail to regenerate in the presence of a continuous aligned astroglial pathway[27]. Thus, in two different *in vivo* models, failure of regeneration was associated with axon-growth arrest at proteoglycan-rich boundaries, rather than at a physical barrier presented by host astrocytes.

Although oligodendrocytes produce factors capable of inhibiting their intrinsic potential to promote axon growth on their own surfaces, the question has remained as to whether they can mask the growth-promoting potential of all other cell types *in vitro*[14,28,29] or *in vivo*. The overall geometry of the intratract astroglia closely paralleled the trajectories of the regenerating axons, suggesting that the intrafascicular astroglia can overcome the inhibitory influence of myelin, at least under the present circumstances (Fig. 3b).

So far we have characterized only one type of neuron in our adult-to-adult transplant model. Intrinsic limitations may contribute to the poor regenerative response of certain subpopulations of mature CNS neurons when confronted with a growth-promoting environment[30]. Irrespective of whether other types of adult neuron can regrow axons in a similar fashion once microtransplanted, we have demonstrated that, once beyond the molecular repulsion associated with a forming glial scar, the adult CNS environment can support regenerative growth from a type of adult neuron that has never before been shown to possess such a remarkable ability to regenerate its axon within adult CNS white matter. □

Methods

Dissociation of dorsal root ganglion neurons. Separate single-cell suspensions of DRG were prepared from adult (250–300 g) and P8 Sprague-Dawley rats. Lumbar and cervical DRGs were dissected, capsules removed, incubated in dispase (5 mg ml^{-1}) and collagenase (100 mg ml^{-1}), and resuspended in 50–100 μl L15 both with CO_2 for maximum cellular density. In some experiments, dissociated cells were preplated to remove adherent non-neuronal cells, and the neuron-enriched supernatant was plated on polylysine/laminin-coated culture plastic overnight in L15-CO_2 with 5% rat serum. Adherent neurons were resuspended in 50–100 μl L15-CO_2, yielding a concentrated and purified neuronal suspension ~1,000 neurons per μl.

Surgical microtransplantation. Adult Sprague-Dawley female rats (200–225 g) were anaesthetized with intramuscular ketamine (100 mg kg^{-1}) and xylazine (2.4 mg kg^{-1}). Stereotactic surgery was done as described[9]. Cell suspensions (0.5 μl) were slowly injected with a picospritzer (General Valve) through a glass micropipette with a bevelled tip and outer and inner diameters of 90 and 70 μm respectively. Thirty-four microtransplants were injected using adult DRG cell suspensions, twenty-six of which contained neurons with normal numbers of satellite cells and eight having small numbers of satellite cells. Seven microtransplants of DRG suspensions from P8 rats with normal satellite cell numbers were also injected. Microtransplants that missed white matter tracts ($n = 4$) were excluded from analysis. Unoperated animals ($n = 2$) and animals with micropipette stabs only ($n = 2$) were used as controls for endogenous CGRP staining in host brains. Following post-operative periods of 2, 4, 6 and 8 days, animals were transcardially perfused with 0.1 M phosphate-buffered saline (PBS) and 4% paraformaldehyde in PBS. Dissected brains were postfixed in 4% paraformaldehyde, and 60-μm Vibratome sections were cut in a modified horizontal plane (parallel to the surface of the cortex) before being processed for immunohistochemical analysis.

Immunohistochemistry. Sections were washed in PBS, blocked with 4% goat serum with 0.1% Triton X-100 in PBS, and incubated overnight with primary antibody in blocking solution followed by secondary and tertiary steps for single, double and triple staining by standard immunocytochemical methods. A polyclonal antibody against CGRP (Accurate; 1:350) was used to identify a subset of DRG neurons. Antibodies against the following antigens were also used: GFAP (Sigma; 1:100), p75 (Boehringer Mannheim; 1:100), myelin/oligodendrocytes (mAb 328; Chemicon; 1:100), chondroitin-6- and -4-sulphate proteoglycans (CS56; Sigma; 1:100), peripherin (Boehringer Mannheim; 1:350). Fluorochromes used to visualize antibody labelling included FITC, Oregon Green, Cy3 and AMCA. Stained sections were examined using a Zeiss laser scanning confocal microscope and a Leitz Orthoplan-2 fluorescence light microscope.

Received 24 June; accepted 18 September 1997.

1. Ramon y Cajal, S. *Degeneration and Regeneration of the Nervous System* (Oxford University Press, London, 1928).
2. Berry, M. *et al*. Deposition of scar tissue in the central nervous system. *Acta Neurochir. Suppl. Wien* **32,** 31–53 (1983).
3. Reier, P. J., Stensaas, L. J. & Guth, L. in *Spinal Cord Reconstruction* (eds Kao, C. C., Bunge, R. P. & Reier, P. J.) 163–195 (Raven, New York, 1983).
4. Rudge, J. S. & Silver, J. Inhibition of neurite outgrowth on astrological scars *in vitro*. *J. Neurosci.* **10,** 3594–3603 (1990).
5. Schwab, M. E., Kapfhammer, J. P. & Bandtlow, C. E. Inhibitors of neurite growth. *Annu. Rev. Neurosci.* **16,** 565–595 (1993).
6. Cheng, H., Cao, Y. & Olson, L. Spinal cord repair in adult paraplegic rats: partial restoration of hind limb function. *Science* **273,** 510–513 (1996).
7. Grill, R., Murai, K., Blesch, A., Gage, F. H. & Tuszynski, M. H. Cellular delivery of neurotrohin-3 promotes corticospinal axonal growth and partial functional recovery after spinal cord injury. *J. Neurosci.* **17,** 5560–5572 (1997).
8. Davies, S. J. A., Field, P. M. & Raisman, G. Long fibre growth by axons of embryonic mouse hippocampal neurons microtransplanted into the adult rat fimbria. *Eur. J. Neurosci.* **5,** 95–106 (1993).
9. Davies, S. J. A., Field, P. M. & Raisman, G. Long interfascicular axon growth from embryonic neurons transplanted into adult myelinated tracts. *J. Neurosci.* **14,** 1596–1612 (1994).
10. Wictorin, K., Brundin, P., Gustavii, B., Lindvall, O. & Bjorklund, A. Reformation of long axon pathways in adult rat central nervous system by human forebrain neuroblasts. *Nature* **347,** 556–558 (1990).
11. Carlstedt, T., Dalsgaard, C. J. & Molander, C. Regrowth of lesioned dorsal root nerve fibers into the spinal cord of neonatal rats. *Neurosci. Lett.* **74,** 14–18 (1987).
12. Gibson, S. J. *et al*. Calcitonin gene-related peptide immunoreactivity in the spinal cord of man and of eight other species. *J. Neurosci.* **4,** 3101–3111 (1984).
13. Bandtlow, C., Zachleder, T. & Schwab, M. E. Oligodendrocytes arrest neurite growth by contact inhibition. *J. Neurosci.* **10,** 3837–3848 (1990).
14. Kobayashi, H., Watanabe, E. & Murikami, F. Growth cones of dorsal root ganglion but not retina collapse and avoid oligodendrocytes in culture. *Dev. Biol.* **168,** 383–394 (1995).
15. Brittis, P. A. & Silver, J. Multiple factors govern intraretinal axon guidance: a time-lapse study. *Mol. Cell. Neurosci.* **6,** 413–432 (1995).
16. Rohrer, H. Nonneuronal cells from chick sympathetic and dorsal root sensory ganglia express catecholamine uptake and receptors for nerve growth factor during development. *Dev. Biol.* **111,** 95–107 (1985).
17. Krekoski, C. A., Parhad, I. M. & Clark, A. W. Attenuation and recovery of nerve growth factor receptor mRNA in dorsal root ganglion neurons following axotomy. *J. Neurosci. Res.* **43,** 1–11 (1996).
18. Snow, D. M., Lemmon, V., Carrino, D. A., Caplan, A. I. & Silver, J. Sulfated proteoglycans in astroglial barriers inhibit neurite outgrowth *in vitro*. *Exp. Neurol.* **109,** 111–130 (1990).
19. Smith-Thomas, L. *et al*. An inhibitor of neurite outgrowth produced by astrocytes. *J. Cell. Sci.* **107,** 1687–1695 (1994).
20. Pindzola, R. R., Doller, C. & Silver, J. Putative inhibitory extracellular matrix molecules at the dorsal root entry zone of the spinal cord during development and after root and sciatic nerve lesions. *Dev. Biol.* **156,** 34–48 (1993).
21. McKeon, R. J., Schreiber, R. C., Rudge, J. S. & Silver, J. Reduction of neurite outgrowth in a model of glial scarring following CNS injury is correlated with the expression of inhibitory molecules on reactive astrocytes. *J. Neurosci.* **11,** 3398–3411 (1991).
22. Lander, A. D. Proteoglycans in the nervous system. *Curr. Opin. Neurobiol.* **3,** 716–723 (1993).
23. Steindler, D. A. *et al*. Boundaries during normal and abnormal brain development: *in vivo* and *in vitro* studies of glia and glycoconjugates. *Exp. Neurol.* **109,** 35–56 (1990).
24. Tessier-Lavigne, M. & Goodman, C. S. The molecular biology of axon guidance. *Science* **274,** 1123–1133 (1996).
25. Giulian, D., Li, J., Li, X., George, J. & Rutecki, P. A. The impact of microglia-derived cytokines upon gliosis in the CNS. *Dev. Neurosci.* **16,** 128–136 (1994).
26. Fitch, M. T. & Silver, J. Activated macrophages and the blood brain barrier: Inflammation after CNS injury leads to increases in putative inhibitory molecules. *Exp. Neurol.* (in the press).
27. Davies, S. J. A., Field, P. M. & Raisman, G. Regeneration of cut adult axons fails even in the presence of continuous aligned glial pathways. *Exp. Neurol.* **142,** 203–216 (1996).
28. Ard, M. D., Bunge, M. B., Wood, P. M., Schachner, M. & Bunge, R. P. Retinal neurite growth on astrocytes is not modified by extracellular matrix, anti-L1 antibody, or oligodendrocytes. *Glia* **4,** 70–82 (1991).
29. Fawcett, J. W., Fersht, N., Housden, L., Schachner, M. & Pesheva, P. Axonal growth on astrocytes is not inhibited by oligodendrocytes. *J. Cell. Sci.* **103,** (1995).
30. Vaudano, E. *et al*. The effects of a lesion or a peripheral nerve graft on GAP-43 upregualtion in the adult rat brain: an *in situ* hybridization and immunocytochemical study. *J. Neurosci.* **15,** 3594–3611 (1995).

Acknowledgements. We thank C. Doller and S. E. MacPhedran for technical assistance. This work was supported by the NIH, the MRC, the Daniel Heumann Fund, the International Spinal Research Trust, the British Neurological Research Trust and the Brumagin Memorial Fund.

Correspondence and requests for material should be addressed to J.S. (e-mail: jxs10@po.cwru.edu).